Memorias del XVI Congreso Latinoamericano de Control Automático, CLCA 2014
Octubre 14-17, 2014. Cancún, Quintana Roo, México

Robust Fault Diagnosis and Accommodation for a Robotic Manipulator under Human Interaction ⋆

Isela Bonilla * **Marco Mendoza** **
Daniel U. Campos-Delgado ***
Andrés A. Valdez-Fernández ****

* *Universidad Autonoma de San Luis Potosi, Facultad de Ciencias, San Luis Potosi, Mexico, (e-mail: ibonilla@fc.uaslp.mx).*
** *(e-mail: marco.mendoza@fc.uaslp.mx)*
*** *(e-mail: ducd@fciencias.uaslp.mx)*
**** *(e-mail: avaldez@fc.uaslp.mx)*

Abstract: This paper addresses the problem of fault diagnosis in a robotic manipulator designed for human interaction. Faults in the external force sensor are addressed with a constant or slowly time-varying profile. A model-based strategy is considered that takes into account uncertainty in the mathematical representation, where a proportional-integral (PI) observer is in charge of estimating the fault profile. This estimation stage incorporates tools from adaptive estimation theory in order to employ in the design stage the uncertainty information, and a compact set of variation for the fault profile. The robotic manipulator includes a nominal control algorithm based on impedance philosophy to address the human-robot interaction. The nominal controller embeds a fault accommodation structure to add fault-tolerance to the closed-loop response. The effectiveness of the proposed approach was verified in simulation under model uncertainty and human-robot interaction, where the results clearly illustrate an accurate fault diagnosis stage and an improved closed-loop response after fault accommodation.

Keywords: Fault diagnosis, fault accommodation, robotic manipulator, observer.

1. INTRODUCTION

The development of automated robotic applications in several industrial and medical processes require contact or human-robot interaction. In fact, safety is an important factor for a successful insertion of robots into human environments. Due to the unstructured nature of the interaction tasks, a robot should be equipped with a complete set of sensors. To ensure the safety of humans interacting with robots during the execution of these tasks, it is important to take into account unexpected events, as failures or abrupt changes of the operating scenario. This condition could affect more the mechanical sensors in the robotic system that suffer constant wearing, for example the devices that measure contact forces. The effect of faults could be more dramatic if the robotic system is working in a closed-loop operation and requires the feedback information of the external forces into the system to regulate properly the human interaction. As a result, the design of tools for diagnosis and reconfiguration of robotic systems under faulty behaviors leads to safer operations. Specifically, a fault diagnosis (FD) scheme is composed by: *fault detection*, that indicates the occurrence of a fault in a monitored system; *fault isolation*, that establishes the type and/or location of the fault; and *fault identification*, that determines the magnitude of the fault (Zhang et al., 2002).

Fault diagnosis methodologies are based on hardware or analytical redundancy. Model-based analytical redundancy have been studied extensively by several research groups: Demetriou and Polycarpou (1998), Zhang et al. (2002), Zhang et al. (2004), Isermann (2006), Espinoza-Trejo et al. (2012), among others. In particular, for interaction tasks, just some FD algorithms have been proposed for fault diagnosis in sensors and/or actuators. Caccavale et al. (2010) suggested a bank of discrete-time model-based observers to detect, isolate and identify failures of joint and force/torque sensors. Muradore and Fiorini (2012) introduced an statistical approach to detect and isolate faults in robotic manipulators, where the diagnostic methodology is based on partial least squares and on the inverse dynamic model of the robot. In (Paviglianiti et al., 2010), an analytical redundancy approach was pursued that relies on a bank of state observers for residual generation. Paviglianiti et al. (2010) adopted an extended $\mathcal{H}_\infty$ approach, and the uncertainty in the model dynamics of each observer was compensated by the use of a radial basis function (RBF) neural network. Despite the widespread interest and relevance of fault diagnosis for robotic systems, only few studies have addressed the problem of robotic manipulation under human interaction, and none that includes fault-tolerant capabilities.

⋆ This research was supported in part by a grant from PROMEP (PROMEP/103.5/12/3953) and CONACYT (# 205782).

Impedance control represents an important tool in interaction tasks that does not rely on an specific force pattern by the manipulator. Instead, the robot adapts its dynamic behavior during the contact robot-human to achieve a desired compliant response. Due to the fact that the mechanical impedance is a relationship between force and motion, the impedance control schemes are widely used in human-robot interaction tasks such as: robotic surgery (Hagn et al., 2008) and rehabilitation therapy (Krebs et al., 2004), (Krebs et al., 2003). In this context, this work presents the design of a robust FD scheme for faults in the external force measurement, which at the same time is capable to accommodate the faulty sensor to compensate the nominal controller based on the impedance framework. The proposed approach is based on the general ideas presented by Zhang et al. (2002), and it considers a FD system to identify and characterize piecewise constant or slowly time-varying faults under human interaction that takes into account model uncertainty. The main goal of our proposal is to guarantee a safety human-robot interaction in a closed-loop framework. In our approach, a Lyapunov direct method is employed to demonstrate the convergence of the fault estimation stage by incorporating tools from adaptive estimation theory. Moreover, a fault-tolerant property is added by considering a fault accommodation structure. Simulation results are presented to validate the mathematical development under a practical scenario and human-robot interaction.

The rest of the paper is organized as follows. First, Section 2 presents the mathematical model of the robotic manipulator and its state-space representation. The impedance control framework is detailed in Section 3, which considers the inverse dynamics of the manipulator and a general potential energy function. Section 4 illustrates the fault modelling for the force sensor, and our proposal for fault diagnosis and accommodation in the closed-loop system. Finally, simulation results for a 2 degrees of freedom robotic manipulator in a 2-dimensional task space is described in Section 5, and the conclusion of this work are drawn in Section 6.

The notation used in this paper is described next. $\mathbb{R}$ denotes real numbers, and $\mathbb{R}^N$ represents real N-dimensional vectors. Scalars are represented by lower-case italic letters, sets by upper-case italic letters, and vector and matrices by boldface letters. $(\cdot)^\top$ describe the transpose of a vector or matrix, $\mathbf{I}$ and $\mathbf{0}$ denote the identity matrix and a vector with zero entries, respectively; and $\text{diag}[x_1, \ldots, x_N]$ a diagonal matrix with entries $(x_1, \ldots, x_N)$. For a vector $\mathbf{x} = [x_1 \ \ldots x_N]^\top$, its Euclidean norm is defined as $\|\mathbf{x}\| = \sqrt{\sum_i |x_i|^2}$. For a matrix $\mathbf{X}$, its minimum and maximum eigenvalues, and 2-norm are denoted as $\lambda_{min}(\mathbf{X})$, and $\lambda_{max}(\mathbf{X})$, and $\|\mathbf{X}\| = \sqrt{\lambda_{max}(\mathbf{X}^\top \mathbf{X})}$, respectively.

2. MATHEMATICAL FORMULATION

The model of a fully actuated robotic manipulator with n degrees of freedom and in an m-dimensional task space can be expressed by the following dynamic equations

$$\mathbf{M}(\mathbf{q})\ddot{\mathbf{q}} + \mathbf{C}(\mathbf{q}, \dot{\mathbf{q}})\dot{\mathbf{q}} + \mathbf{g}(\mathbf{q}) + \mathbf{F}\dot{\mathbf{q}} = \boldsymbol{\tau} - \mathbf{J}^\top(\mathbf{q})\mathbf{f}_{ext} \quad (1)$$

where $\mathbf{q} \in \mathbb{R}^n$, $\boldsymbol{\tau} \in \mathbb{R}^n$, $\mathbf{f}_{ext} \in \mathbb{R}^m$ denote the vectors of joint displacements, input torques, and external and interaction forces; meanwhile $\mathbf{M}(\mathbf{q}) \in \mathbb{R}^{n\times n}$, $\mathbf{C}(\mathbf{q}, \dot{\mathbf{q}}) \in \mathbb{R}^{n\times n}$, $\mathbf{J}(\mathbf{q}) \in \mathbb{R}^{m\times n}$ and $\mathbf{F} \in \mathbb{R}^{n\times n}$ ($\mathbf{F} > 0$) stand for the inertia, coriolis, jacobian and viscous friction matrices, and $g(\mathbf{q}) \in \mathbb{R}^n$ for the vector of gravity forces. The dynamic model in (1) can be written in the following state-space representation:

$$\dot{\mathbf{x}} = \mathbf{f}(\mathbf{x}, \mathbf{u}) + \mathbf{h}(\mathbf{x})\mathbf{f}_{ext} + \boldsymbol{\eta}(\mathbf{x}, \mathbf{u}) \quad (2)$$

where $\mathbf{x} = [\mathbf{x}_1, \mathbf{x}_2]^\top \in \mathbb{R}^{2n}$ is the state vector with components $\mathbf{x}_1 = \mathbf{q}$ and $\mathbf{x}_2 = \dot{\mathbf{q}}$, $\mathbf{u} = \boldsymbol{\tau}$ is the input vector,

$$\mathbf{f}(\mathbf{x}, \mathbf{u}) = \begin{bmatrix} \mathbf{x}_2 \\ \mathbf{M}^{-1}(\mathbf{x}_1)\{-\mathbf{C}(\mathbf{x}_1, \mathbf{x}_2)\mathbf{x}_2 - \mathbf{F}\mathbf{x}_2 - \mathbf{g}(\mathbf{x}_1) + \mathbf{u}\} \end{bmatrix},$$
$$\mathbf{h}(\mathbf{x}) = \begin{bmatrix} \mathbf{0} \\ -\mathbf{M}^{-1}(\mathbf{x}_1)\mathbf{J}^\top(\mathbf{x}_1) \end{bmatrix}, \quad (3)$$

and $\boldsymbol{\eta}(\mathbf{x}, \mathbf{u}) \in \mathbb{R}^{2n}$ denotes a vector field of model uncertainty which is assumed bounded by a known and smooth function

$$\|\boldsymbol{\eta}(\mathbf{x}, \mathbf{u})\| \leq \bar{\eta}(\mathbf{x}, \mathbf{u}) \quad \forall (\mathbf{x}, \mathbf{u}) \in \Omega, \quad (4)$$

where $\Omega \subset \mathbb{R}^{2n} \times \mathbb{R}^n$ defines the operating region. In (2), all the states $\mathbf{x}$, and external and interaction forces $\mathbf{f}_{ext}$ are assumed available for feedback. Furthermore, all the parameters in the model (2) are supposed to be identified off-line previously.

3. IMPEDANCE CONTROL ACTION

The impedance-control framework used in this paper corresponds to a generalization of motion control in task-space, and it was proposed by Bonilla et al. (2011). The main goal of this impedance controller is

$$\lim_{t\to\infty} \tilde{\boldsymbol{\xi}}(t) = \mathbf{0} \quad (5)$$

where

$$\tilde{\boldsymbol{\xi}} = \tilde{\mathbf{p}} - \mathbf{p}_{f_{ext}} \quad (6)$$

with $\tilde{\mathbf{p}} = \mathbf{p}_d - \mathbf{p}$ representing the unconstrained tracking error, and $\mathbf{p}_d \in \mathbb{R}^m$ and $\mathbf{p} \in \mathbb{R}^m$ being the desired and actual robot end-effector position vectors, respectively, in the operational Cartesian space. Whereas, $\mathbf{p}_{f_{ext}} = [\mathbf{M}_d s^2 + \mathbf{B}_d s + \mathbf{K}_d]^{-1}\mathbf{f}_{ext}$ represents the external filtered force which is employed to obtain a position adjustment, if human-robot interaction is induced. The filtered force $\mathbf{p}_{f_{ext}}$ is constructed by tuning the impedance parameters $\mathbf{K}_d \in \mathbb{R}^{m\times m}$ (stiffness), $\mathbf{B}_d \in \mathbb{R}^{m\times m}$ (damping) and $\mathbf{M}_d \in \mathbb{R}^{m\times m}$ (inertia), where all the parameters are symmetric positive definite matrices. Note that, in absence of contact, i.e. if $\mathbf{f}_{ext} \equiv \mathbf{0}$, the objective of impedance control is equivalent to the objective of motion control in task-space. Therefore, this approach to impedance control can be seen as a motion-control approach allowing a tolerance to error in the tracking of the desired trajectory in the presence of interaction forces. Considering the definition of impedance error in (6), the vectors

$$\dot{\tilde{\boldsymbol{\xi}}} = \dot{\mathbf{p}}_d - \dot{\mathbf{p}} - \dot{\mathbf{p}}_{f_{ext}} \quad (7)$$
$$\ddot{\tilde{\boldsymbol{\xi}}} = \ddot{\mathbf{p}}_d - \ddot{\mathbf{p}} - \ddot{\mathbf{p}}_{f_{ext}} \quad (8)$$

represent the first and second time derivatives of the impedance error, respectively. The global control structure

is based on the concept of inverse dynamics, where the robot torques are selected as

$$\boldsymbol{\tau} = \mathbf{M}(\mathbf{q})\mathbf{J}^{-1}(\mathbf{q})[\mathbf{a} - \dot{\mathbf{J}}(\mathbf{q})\dot{\mathbf{q}}] + \mathbf{C}(\mathbf{q},\dot{\mathbf{q}})\dot{\mathbf{q}} + \mathbf{g}(\mathbf{q}) + \mathbf{F}\dot{\mathbf{q}} + \mathbf{J}^{\top}(\mathbf{q})\mathbf{f}_{ext}, \quad (9)$$

where $\mathbf{a} \in \mathbb{R}^m$ is a complementary control action. In order to satisfy the impedance-control objective (5), several controllers can be derived by defining an artificial potential energy function $\mathcal{U}_p : \mathbb{R}^m \mapsto \mathbb{R}$ such that

- $\mathcal{U}_p(\tilde{\boldsymbol{\xi}}) > 0$, and $\mathcal{U}_p(\tilde{\boldsymbol{\xi}}) \equiv 0 \iff \tilde{\boldsymbol{\xi}} = \mathbf{0}\ \forall \tilde{\boldsymbol{\xi}} \in \mathbb{R}^m$,
- $\tilde{\boldsymbol{\xi}}^{\top}\nabla\mathcal{U}_p(\tilde{\boldsymbol{\xi}}) > 0$, and $\tilde{\boldsymbol{\xi}}^{\top}\nabla\mathcal{U}_p(\tilde{\boldsymbol{\xi}}) \equiv 0 \iff \tilde{\boldsymbol{\xi}} = \mathbf{0}$, $\forall \tilde{\boldsymbol{\xi}} \in \mathbb{R}^m$,
- $\nabla\mathcal{U}_p(\tilde{\boldsymbol{\xi}}) \equiv \mathbf{0} \iff \tilde{\boldsymbol{\xi}} = \mathbf{0}$,

where $\nabla\mathcal{U}_p(\tilde{\boldsymbol{\xi}})$ is the gradient of $\mathcal{U}_p$. Then, the complementary control action $\mathbf{a}$ can be written as

$$\mathbf{a} = \ddot{\mathbf{p}}_d - \ddot{\mathbf{p}}_{f_{ext}} + \mathbf{M}_d^{-1}[\nabla\mathcal{U}_p(\tilde{\boldsymbol{\xi}}) + \mathbf{K}_v\dot{\tilde{\boldsymbol{\xi}}}] \quad (10)$$

such that the origin of the closed-loop system is asymptotically stable in the Lyapunov sense (Bonilla et al., 2011), where $\mathbf{K}_v \in \mathbb{R}^{m\times m}$ is a diagonal positive-definite matrix of derivative gains. An example of the artificial potential energy function that is employed in this work is

$$\mathcal{U}_p(\tilde{\boldsymbol{\xi}}) = \frac{1}{2}\tilde{\boldsymbol{\xi}}^{\top}\mathbf{K}_p\tilde{\boldsymbol{\xi}}$$

where $\mathbf{K}_p \in \mathbb{R}^{m\times m}$ is a diagonal positive-definite matrix of proportional gains. With this energy function, it is obtained that

$$\nabla\mathcal{U}_p(\tilde{\boldsymbol{\xi}}) = \mathbf{K}_p\tilde{\boldsymbol{\xi}}$$

then

$$\mathbf{a} = \ddot{\mathbf{p}}_d - \ddot{\mathbf{p}}_{f_{ext}} + \mathbf{M}_d^{-1}[\mathbf{K}_p\tilde{\boldsymbol{\xi}} + \mathbf{K}_v\dot{\tilde{\boldsymbol{\xi}}}], \quad (11)$$

and thus it can be observed that $\mathbf{K}_p\tilde{\boldsymbol{\xi}} + \mathbf{K}_v\dot{\tilde{\boldsymbol{\xi}}}$ represents a proportional-derivative (PD) control action.

4. FAULT DIAGNOSIS AND ACCOMMODATION

4.1 Fault Modeling

In our formulation, the robotic manipulator is assumed to work under a closed-loop structure that allows human interaction. For this purpose, it is crucial the feedback information from the external and interaction forces $\mathbf{f}_{ext}$. Due to continuous wearing and ageing, the mechanical sensor responsible for this measurement $\mathbf{f}_{ext}$ could face faults, and its incorrect or erroneous information could have a negative effect in the interaction regimes. Therefore, we study a fault diagnosis technique that could detect and identify this condition by assuming an additive model and a piece-wise constant or slowly time-varying profile for the fault, i.e.

$$\hat{\mathbf{f}}_{ext} = \mathbf{f}_{ext} + \Delta\mathbf{f}_{ext} \quad (12)$$

where $\hat{\mathbf{f}}_{ext}$ represents the measured external force, and $\Delta\mathbf{f}_{ext}$ the induced fault, where $d\Delta\mathbf{f}_{ext}/dt \approx 0$ (almost everywhere with exception of points in a zero measure set) after fault triggering and $\Delta\mathbf{f}_{ext} = 0$ in a healthy condition. For any time, the fault profile $\Delta\mathbf{f}_{ext}$ is assumed to belong to a compact set $U \subset \mathbb{R}^m$. In addition, it is assumed that after the fault, the closed-loop control could still preserve a bounded operation, and as a consequence, the assignation of the operating region Ω to limit the uncertain terms in (4) is feasible.

4.2 Fault Diagnosis

For fault detection and identification, a PI observer that incorporates concepts from adaptive estimation theory is proposed to estimate $\Delta\mathbf{f}_{ext}$ after fault triggering (Ioannou and Fidan, 2006). In order to provide a robust diagnosis stage, the uncertainty bound in (4) is employed to derive adaptive thresholds for fault detection. First, the proposed observer has the following dynamic structure

$$\begin{aligned}\dot{\hat{\mathbf{x}}} &= \boldsymbol{\Lambda}(\mathbf{x} - \hat{\mathbf{x}}) + \mathbf{f}(\mathbf{x},\mathbf{u}) + \mathbf{h}(\mathbf{x})\{\hat{\mathbf{f}}_{ext} - \mathbf{w}\}\\ \dot{\mathbf{w}} &= \Phi\{-\boldsymbol{\Gamma}\mathbf{h}^{\top}(\mathbf{x})(\mathbf{x} - \hat{\mathbf{x}})\}\end{aligned} \quad (13)$$

where $\hat{\mathbf{x}} \in \mathbb{R}^{2n}$ is the estimated state vector, $\boldsymbol{\Lambda} \in \mathbb{R}^{2n\times 2n}$ is a diagonal positive definite matrix, $\boldsymbol{\Gamma} \in \mathbb{R}^{m\times m}$ represents the learning rate matrix which is positive definite, $\mathbf{w} \in \mathbb{R}^m$ denotes the estimation of the fault component $\Delta\mathbf{f}_{ext}$, and $\Phi : \mathbb{R}^m \mapsto U$ represents a projection operator into its feasible set U (Zhang et al., 2002) (Ioannou and Fidan, 2006). Since in the control of robotic manipulators with human interaction (Bonilla et al., 2011), the state vector $\mathbf{x}$ is usually available for feedback, the implementation of the observer in (13) is viable in practice. Therefore, in the case of a healthy system and no-uncertainty, the error dynamics $\mathbf{e}_{\mathbf{x}} = \mathbf{x} - \hat{\mathbf{x}}$ and $\mathbf{e}_{\mathbf{w}} = \Delta\mathbf{f}_{ext} - \mathbf{w}$ are given by

$$\begin{aligned}\dot{\mathbf{e}}_{\mathbf{x}} &= -\boldsymbol{\Lambda}\mathbf{e}_{\mathbf{x}} & \mathbf{e}_{\mathbf{x}}(0) &= \mathbf{e}_0\\ \dot{\mathbf{e}}_{\mathbf{w}} &= \Phi\{\boldsymbol{\Gamma}\mathbf{h}^{\top}(\mathbf{x})\mathbf{e}_{\mathbf{x}}\} & \mathbf{e}_{\mathbf{w}}(0) &= \mathbf{0}.\end{aligned} \quad (14)$$

for any initial condition $\mathbf{e}_0 \in \mathbb{R}^{2n}$. Then, the origin $(\mathbf{0},\mathbf{0})$ is an equilibrium of the error system, where the resulting dynamics in (14) are time-invariant. In order to determine an adaptive threshold for fault detection, it is assumed a time instant $T > 0$ such that the effect of the initial condition has disappeared, and define a new time index $t' = t - T$, such that the error $\mathbf{e}_{\mathbf{x}}$ is at the origin for $t' = 0$. Then, taking into account model uncertainty, the error model is now described by

$$\begin{aligned}\dot{\mathbf{e}}_{\mathbf{x}} &= -\boldsymbol{\Lambda}\mathbf{e}_{\mathbf{x}} + \boldsymbol{\eta}(\mathbf{x},\mathbf{u}) \qquad \forall t' \geq 0\\ \Rightarrow \mathbf{e}_{\mathbf{x}}(t') &= \int_0^{t'} e^{-\boldsymbol{\Lambda}(t'-\sigma)}\boldsymbol{\eta}(\mathbf{x}(\sigma),\mathbf{u}(\sigma))d\sigma\end{aligned} \quad (15)$$

and since $\boldsymbol{\Lambda}$ is diagonal positive definite, it is satisfied $\|e^{-\boldsymbol{\Lambda}t'}\| \leq e^{-\lambda_m t'}$, where $\lambda_m \triangleq \min_i\{\lambda_i\} > 0$ is the diagonal entry with the lowest value in $\boldsymbol{\Lambda}$. As a result, the following upper-bound is reached for the error vector

$$\|\mathbf{e}_{\mathbf{x}}(t')\| \leq \underbrace{\int_0^{t'} e^{-\lambda_m(t'-\sigma)}\bar{\eta}(\mathbf{x}(\sigma),\mathbf{u}(\sigma))d\sigma}_{\epsilon(t')} \quad \forall t' \geq 0 \quad (16)$$

Consequently, $\epsilon(t')$ represents an adaptive threshold on the estimation error related to the upper-bound on the model uncertainty. Hence in order to add robustness to the observer in (13), a dead-zone function $\mathrm{D} : \mathbb{R}^{2n} \mapsto \mathbb{R}^{2n}$ with an adaptive threshold is proposed as follows

$$\dot{\mathbf{w}} = \Phi\{-\boldsymbol{\Gamma}\mathbf{h}^{\top}(\mathbf{x})\mathrm{D}(\mathbf{e}_{\mathbf{x}})\} \qquad \forall t' \geq 0 \quad (17)$$

where

$$\mathrm{D}(\mathbf{e}_{\mathbf{x}}) = \begin{cases}\mathbf{0} & \|\mathbf{e}_{\mathbf{x}}(t')\| \leq \epsilon(t')\\ \mathbf{e}_{\mathbf{x}}(t') & \|\mathbf{e}_{\mathbf{x}}(t')\| > \epsilon(t')\end{cases} \quad (18)$$

In this way, if the estimation error $\mathbf{e}_{\mathbf{x}}$ does not exceeds the threshold $\epsilon(t')$, the integral correction $\mathbf{w}$ in (17) is not activated in a healthy condition.

Now, after the fault appears at time $t' = T_{fault} > 0$, the resulting error dynamics will be given by

$$\dot{\mathbf{e}}_{\mathbf{x}} = -\mathbf{\Lambda}\mathbf{e}_{\mathbf{x}} - \mathbf{h}(\mathbf{x})\mathbf{e}_{\mathbf{w}} + \boldsymbol{\eta}(\mathbf{x},\mathbf{u})$$
$$\dot{\mathbf{e}}_{\mathbf{w}} = \Phi\{\mathbf{\Gamma}\mathbf{h}^{\top}(\mathbf{x})\mathrm{D}(\mathbf{e}_{\mathbf{x}})\} \quad (19)$$

Therefore, the error convergence is analyzed through a Lyapunov function

$$V = \frac{1}{2}\mathbf{e}_{\mathbf{x}}^{\top}\mathbf{e}_{\mathbf{x}} + \frac{1}{2}\mathbf{e}_{\mathbf{w}}^{\top}\mathbf{\Gamma}^{-1}\mathbf{e}_{\mathbf{w}} \quad (20)$$

whose time derivative is given by

$$\dot{V} = -\mathbf{e}_{\mathbf{x}}^{\top}\mathbf{\Lambda}\mathbf{e}_{\mathbf{x}} - \mathbf{e}_{\mathbf{x}}^{\top}\mathbf{h}(\mathbf{x})\mathbf{e}_{\mathbf{w}} + \mathbf{e}_{\mathbf{x}}^{\top}\boldsymbol{\eta}(\mathbf{x},\mathbf{u}) + \mathbf{e}_{\mathbf{w}}^{\top}\mathbf{\Gamma}^{-1}\Phi\{\mathbf{\Gamma}\mathbf{h}^{\top}(\mathbf{x})\mathrm{D}(\mathbf{e}_{\mathbf{x}})\}. \quad (21)$$

Next, if it is assumed that $\mathbf{\Gamma}\mathbf{h}^{\top}(\mathbf{x})\mathrm{D}(\mathbf{e}_{\mathbf{x}}) \in U$, then

$$\dot{V} = -\mathbf{e}_{\mathbf{x}}^{\top}\mathbf{\Lambda}\mathbf{e}_{\mathbf{x}} + \mathbf{e}_{\mathbf{x}}^{\top}\boldsymbol{\eta}(\mathbf{x},\mathbf{u}) - \mathbf{e}_{\mathbf{w}}^{\top}\mathbf{h}^{\top}(\mathbf{x})\{\mathbf{e}_{\mathbf{x}} - \mathrm{D}(\mathbf{e}_{\mathbf{x}})\}, \quad (22)$$

and an inequality on the time derivative of the Lyapunov function is deduced

$$\dot{V} \leq -\lambda_m\|\mathbf{e}_{\mathbf{x}}\|^2 + \|\mathbf{e}_{\mathbf{x}}\|\|\boldsymbol{\eta}(\mathbf{x},\mathbf{u})\| - \mathbf{e}_{\mathbf{w}}^{\top}\mathbf{h}^{\top}(\mathbf{x})\{\mathbf{e}_{\mathbf{x}} - \mathrm{D}(\mathbf{e}_{\mathbf{x}})\} \quad (23)$$
$$\leq -\|\mathbf{e}_{\mathbf{x}}\|(\lambda_m\|\mathbf{e}_{\mathbf{x}}\| - \omega) - \mathbf{e}_{\mathbf{w}}^{\top}\mathbf{h}^{\top}(\mathbf{x})\{\mathbf{e}_{\mathbf{x}} - \mathrm{D}(\mathbf{e}_{\mathbf{x}})\} \quad (24)$$

where due to the boundedness of $\mathbf{x}$ and $\mathbf{u}$, and smoothness of the upper-bound uncertainty term $\bar{\eta}(\mathbf{x},\mathbf{u})$, then there exists a constant $\omega > 0$ such that $\omega = \sup_{(\mathbf{x},\mathbf{u})\in\Omega}\bar{\eta}(\mathbf{x},\mathbf{u})$. Now, from (16) and the previous definition, the following inequality is derived

$$\|\mathbf{e}_{\mathbf{x}}(t')\| \leq \epsilon(t') \leq \frac{\omega}{\lambda_m}(1 - e^{-\lambda_m t}) \leq \frac{\omega}{\lambda_m} \qquad \forall t' \geq 0. \quad (25)$$

Hence if $\|\mathbf{e}_{\mathbf{x}}\| > \frac{\omega}{\lambda_m}$, then $\mathbf{e}_{\mathbf{x}} - \mathrm{D}(\mathbf{e}_{\mathbf{x}}) = 0$, since the zero value of the dead-zone could be overcome all the time. Consequently, from (24) and (25), the time derivative of the Lyapunov functions satisfies

$$\|\mathbf{e}_{\mathbf{x}}\| > \frac{\omega}{\lambda_m} \;\Rightarrow\; \dot{V} \leq 0. \quad (26)$$

Furthermore, by LaSalle's theorem (Khalil, 2002), in the case of no uncertainty, if $\mathbf{e}_{\mathbf{x}} = 0$ then by (19), convergence of the fault estimation is guaranteed $\mathbf{e}_{\mathbf{w}} \to 0$.

4.3 Fault Accommodation

Finally, after fault detection, and after some adaptation time regulated by matrix $\mathbf{\Lambda}$, the fault could be identified by the observer in (13). This information can then be used by the nominal impedance control action described in Section 3, in order to improve the human-interaction by adding a fault-tolerant capability to the closed-loop response (Isermann, 2006), (Zhang et al., 2004). Therefore, the force filtering was now implemented as $\mathbf{p}_{f_{ext}} = [s^2\mathbf{M}_d + s\mathbf{B}_d + \mathbf{K}_d]^{-1}(\hat{\mathbf{f}}_{ext} - \mathbf{w})$ to incorporate the estimation in $\mathbf{w}$ to accommodate the fault.

5. SIMULATION EVALUATION

In this section, some simulation results that validate the effectiveness of the proposed fault diagnosis and accommodation scheme in Fig. 1 are presented.

5.1 Robotic System

The robot corresponds to a serial link manipulator with two degrees of freedom ($n = 2$) in a 2-dimensional task-space ($m = 2$), i.e. $\mathbf{q} = [q_1 \;\; q_2]^{\top}$, $\dot{\mathbf{q}} = [\dot{q}_1 \;\; \dot{q}_2]^{\top}$ and $\mathbf{f}_{ext} = [f_{ext_1} \; f_{ext_2}]^{\top}$. The robot parameters were reported in Reyes and Kelly (1997), so the corresponding elements of the dynamical model (1) are defined as follows. First, the manipulator inertia, and the coriolis and centripetal acceleration matrices are given by

$$\mathbf{M}(\mathbf{q}) = \begin{bmatrix} 2.351 + 2(0.084)\cos(q_2) & 0.102 + 0.084\cos(q_2) \\ 0.102 + 0.084\cos(q_2) & 0.102 \end{bmatrix} [\mathrm{Nm}\cdot\mathrm{s}^2/\mathrm{rad}],$$

$$\mathbf{C}(\mathbf{q},\dot{\mathbf{q}}) = \begin{bmatrix} -2(0.084)\sin(q_2)\dot{q}_2 & -0.084\sin(q_2)\dot{q}_2 \\ 0.084\sin(q_2)\dot{q}_1 & 0.0 \end{bmatrix} [\mathrm{Nm}\cdot\mathrm{s}/\mathrm{rad}],$$

the vector of gravitational force is expressed as

$$\mathbf{g}(\mathbf{q}) = \begin{bmatrix} 38.465\sin(q_1) + 1.825\sin(q_1+q_2) \\ 1.825\sin(q_1+q_2) \end{bmatrix} [\mathrm{Nm}],$$

whereas the vector due to viscous friction is described by

$$\mathbf{F}\dot{\mathbf{q}} = \begin{bmatrix} 2.288\,\dot{q}_1 \\ 0.175\,\dot{q}_2 \end{bmatrix} [\mathrm{Nm}].$$

Finally, the Jacobian matrix of the manipulator is given by

$$\mathbf{J}(\mathbf{q}) = \begin{bmatrix} l(\cos(q_1) + \cos(q_1+q_2)) & l\cos(q_1+q_2) \\ l(\sin(q_1) + \sin(q_1+q_2)) & l\sin(q_1+q_2) \end{bmatrix} [\mathrm{m}]$$

where l =0.45 m. The uncertainty term $\boldsymbol{\eta}(\mathbf{x},\mathbf{u})$ in the simulation test corresponds to Coulomb friction torques

$$\boldsymbol{\eta}(\mathbf{x},\mathbf{u}) = \begin{bmatrix} 0 \\ 0 \\ f_{C1}\,\mathrm{sign}(x_3) \\ f_{C2}\,\mathrm{sign}(x_4) \end{bmatrix} [\mathrm{Nm}]$$

where

$$f_{C1} = \begin{cases} 7.170 & \text{if } x_3 > 0 \\ 8.049 & \text{if } x_3 < 0 \end{cases}$$
$$f_{C2} = 1.734,$$

where $x_1 = q_1$, $x_2 = q_2$, $x_3 = \dot{q}_1$ and $x_4 = \dot{q}_2$. Consequently, the following upper-bound function of the uncertainty term is selected as

$$\bar{\eta}(\mathbf{x},\mathbf{u}) = \begin{cases} 10.0 & x_3 \notin \Upsilon \;\wedge\; x_4 \notin \Upsilon \\ 9.8 & x_3 \notin \Upsilon \;\wedge\; x_4 \in \Upsilon \\ 2.0 & x_3 \in \Upsilon \;\wedge\; x_4 \notin \Upsilon \\ 0 & x_3 \in \Upsilon \;\wedge\; x_4 \in \Upsilon \end{cases} \quad (27)$$

where $\Upsilon = [-\epsilon, \epsilon]$ is a neighbourhood of the origin, with $\epsilon > 0$ in order to avoid constant switching due to measurement noise. To simulate the human-robot interaction, the following time profile was used for the external interaction force

$$f_{ext_i} = 30\tanh(0.2t)\ [\mathrm{N}] \qquad \forall t \geq 0,\ i \in \{1,2\}.$$

A typical behavior of the norm of the impedance error $\|\tilde{\boldsymbol{\xi}}\|$ in a healthy case, *i.e.* in absence of a fault in the external force measurement, is presented in Fig. 2. In this plot, it can be observed an accurate regulation according with the objective in (5).

5.2 Fault Diagnosis Test

In order to safely simulate the presence of a force-sensor fault, a constant signal (polarization fault) was added to

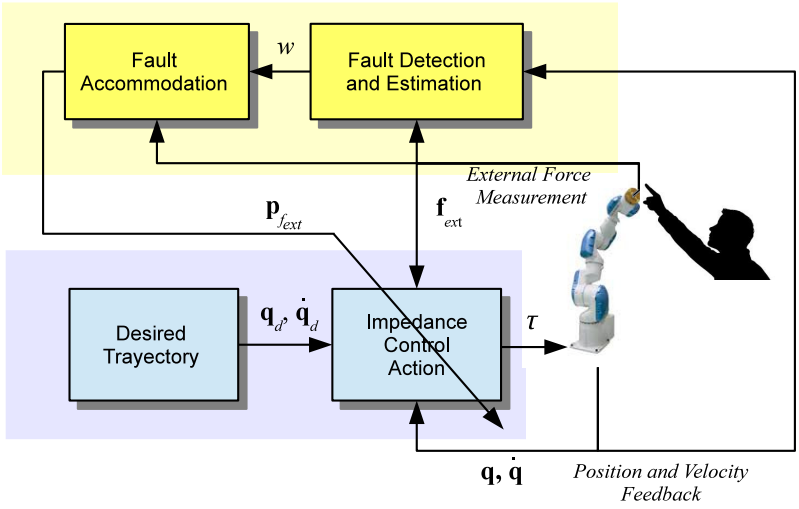

Fig. 1. Block Diagram of Fault Diagnosis and Accommodation Scheme.

the measured external force signal after fault triggering. A fault occurrence at $T_{fault} = 2$ seconds was considered and it is characterized by the following constant vector

$$\Delta \mathbf{f}_{ext} = \begin{bmatrix} 10.0 \\ 8.0 \end{bmatrix} \text{ [N]}. \tag{28}$$

The positive-definite PI-gain matrices in the diagnostic observer in (13) and (17) were chosen as

$$\begin{aligned} \mathbf{\Lambda} &= \text{diag}[450, 200, 250, 350] \\ \mathbf{\Gamma} &= \text{diag}[18585, 10510]. \end{aligned} \tag{29}$$

by trial and error in order to achieve a fast transient response in the estimation process, and with a diagonal structure for simplicity. For detection purposes, and to simplify the evaluation, a constant threshold of 0.05 was used, *i.e.* $\|\mathbf{e_x}\| > 0.05$ if a fault appears, since $\omega = 10$ and $\lambda_m = 200$ according to (27) and (29). Figure 3 shows the estimates of the polarization fault, where the top plots shows the estimated first component of the fault profile Δf_{ext_1}, and in the bottom, the estimated second one Δf_{ext2}. This plot shows that both estimations reach the simulated values in (28) with a fast transient behavior.

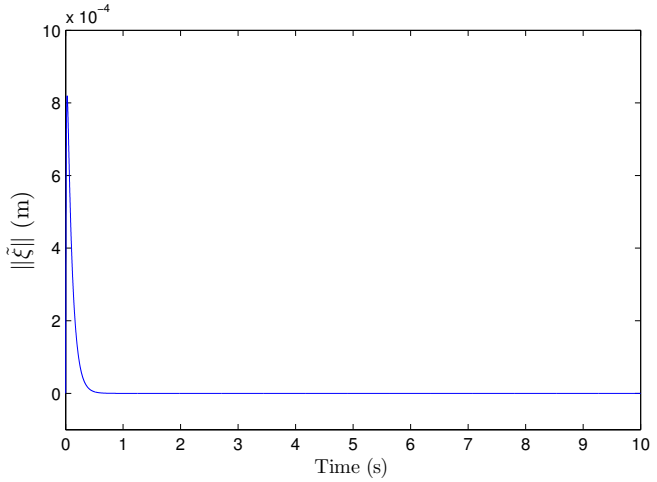

Fig. 2. Norm of the impedance error $\|\tilde{\boldsymbol{\xi}}\|$ in a healthy case.

Now, in order to study the response of the closed-loop system when the fault appears, the force filtering was implemented first by just the faulty measurement as $\mathbf{p}_{f_{ext}} = [s^2\mathbf{M}_d + s\mathbf{B}_d + \mathbf{K}_d]^{-1}\hat{\mathbf{f}}_{ext}$, that includes the effect of polarization $\Delta \mathbf{f}_{ext}$. In this case, the norm of the impedance error increases (after fault triggering at 2 sec.), as can be seen in Fig. 4. To improve the closed-loop performance, the fault accommodation scheme described in Section 4.3 was implemented. Figure 5 shows the behavior of the impedance error, so after the fault appears (at 2 sec.) the error tends to zero, minimizing the undesired effect caused by the polarization fault, compared to Fig. 4. The steady-state value of the impedance error, in the case of Fig. 5, can be minimized by a proper tuning of the observer gain matrices $\mathbf{\Lambda}$ and $\mathbf{\Gamma}$, in order to improve the fault estimation.

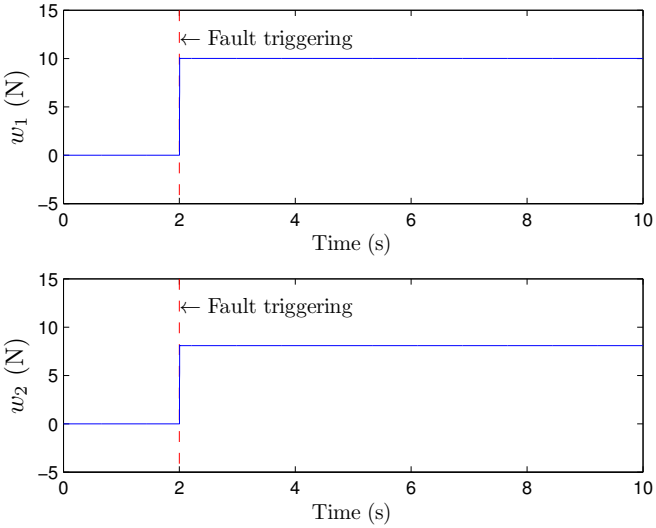

Fig. 3. Estimates of the force sensor fault with triggering time $T_{fault} = 2$ seconds.

6. CONCLUSIONS

In this paper, a robust fault diagnosis and accommodation scheme for human-robot interaction systems has been presented. The proposed approach looks to guarantee a safety human-robot interaction by combining a model-based observer with an adaptive integral action for fault estimation

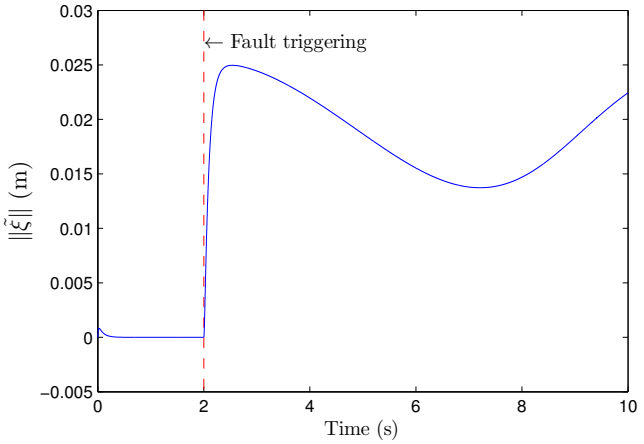

Fig. 4. Norm of the impedance error after a fault condition with triggering time $T_{fault} = 2$ seconds.

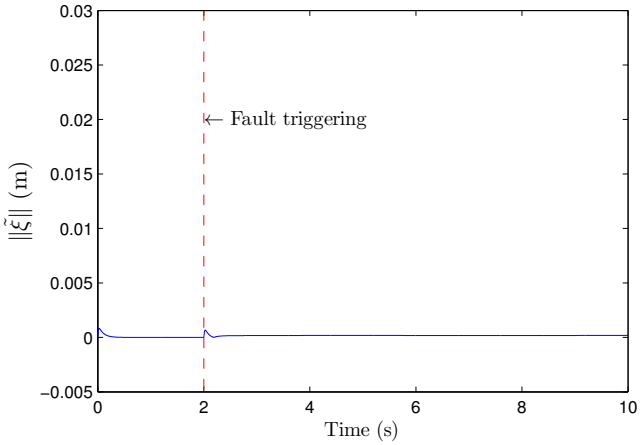

Fig. 5. Norm of the impedance error when the fault is accommodated after triggering at $T_{fault} = 2$ seconds.

purposes. Also, the scheme takes into account uncertainty in the robot model, providing robustness into the overall strategy. The convergence of the fault estimation process has been proved by using Lyapunov's direct method and LaSalle's theorem. A nominal closed-loop controller based on the impedance philosophy was considered to address the human-robot interaction. In order to incorporate fault tolerance into the approach, the estimated fault is accommodated into the nominal control algorithm. A simulation evaluation was presented to initially validate the proposal that includes model uncertainty, where the obtained results illustrate an accurate fault diagnosis stage, and an improved performance after fault triggering in the closed-loop response due to fast accommodation. As part of the ongoing research work, we will validate experimentally this proposal, consider more elaborated testing scenarios for the human-robot interaction, and study fault diagnosis and accommodation for the angular position sensors.

REFERENCES

Bonilla, I., Reyes, F., Mendoza, M., and González-Galván, E.J. (2011). A dynamic-compensation approach to impedance control of robot manipulators. *Journal of Intelligent & Robotic Systems*, 63(1), 51–73.

Caccavale, F., Marino, A., and Pierri, F. (2010). Sensor fault diagnosis for manipulators performing interaction tasks. In *2010 IEEE International Symposium on Industrial Electronics (ISIE 2010)*, 2121–2126.

Demetriou, M. and Polycarpou, M. (1998). Incipient fault diagnosis of dynamical systems using online approximators. *IEEE Trans. on Automatic Control*, 43, 1612–1617.

Espinoza-Trejo, D., Campos-Delgado, D., Barcenas, E., and Martínez-López, F. (2012). Robust fault diagnosis scheme for open-circuit faults in voltage source inverters feeding induction motors by using non-linear proportional-integral observers. *IET Power Electronics*, 5(7), 1204–1216.

Hagn, U., Nickl, M., Jorg, S., Passig, G., Bahls, T., Nothhelfer, A., Hacker, F., Le-Tien, L., Albu-Schaffer, A., Konietschke, R., Grebenstein, M., Warpup, R., Haslinger, R., Frommberger, M., and Hirzinger, G. (2008). The dlr miro: A versatile lightweight robot for surgical applications. *Industrial Robot: An International Journal*, 35, 324–336.

Ioannou, P. and Fidan, B. (2006). *Adaptive Control Tutorial*. Society for Industrial and Applied Mathematics, first edition.

Isermann, R. (2006). *Fault-Diagnosis Systems: An Introduction from Fault Detection to Fault Tolerance*. Springer, Berlin.

Khalil, H. (2002). *Nonlinear Systems*. Prentice Hall, Upper Saddle River, New Jersey, third edition.

Krebs, H., Ferraro, M., Buerger, S., Newbery, M., Makiyama, A., Sandmann, M., Lynch, D., Volpe, B., and Hogan, N. (2004). Rehabilitation robotics: pilot trial of a spatial extension for mit-manus. *Journal of NeuroEngineering and Rehabilitation*, 1, 1–15.

Krebs, H., Volpe, B., Aisen, M., Hening, W., Adamovich, S., Poizner, H., Subrahmanyan, K., and Hogan, N. (2003). Robotic applications in neuromotor rehabilitation. *Robotica*, 21, 3–11.

Muradore, R. and Fiorini, P. (2012). A pls-based statistical approach for fault detection and isolation of robotic manipulators. *Industrial Electronics, IEEE Transactions on*, 59(8), 3167–3175.

Paviglianiti, G., Pierri, F., Caccavale, F., and Mattei, M. (2010). Robust fault detection and isolation for proprioceptive sensors of robot manipulators. *Mechatronics*, 20(1), 162–170.

Reyes, F. and Kelly, R. (1997). Experimental evaluation of identification schemes on a direct drive robot. *Robotica*, 15(5), 563–571.

Zhang, X., Parisini, T., and Polycarpou, M. (2004). Adaptive fault-tolerant control of nonlinear uncertain systems: An informatic-based diagnostic approach. *IEEE Trans. on Automatic Control*, 49, 1259–1274.

Zhang, X., Polycarpou, M., and Parisini, T. (2002). A robust detection and isolation scheme for abrupt and incipient faults in nonlinear systems. *IEEE Trans. on Automatic Control*, 47, 576–593.